

PCCP

Accepted Manuscript



This is an *Accepted Manuscript*, which has been through the Royal Society of Chemistry peer review process and has been accepted for publication.

Accepted Manuscripts are published online shortly after acceptance, before technical editing, formatting and proof reading. Using this free service, authors can make their results available to the community, in citable form, before we publish the edited article. We will replace this *Accepted Manuscript* with the edited and formatted *Advance Article* as soon as it is available.

You can find more information about *Accepted Manuscripts* in the [Information for Authors](#).

Please note that technical editing may introduce minor changes to the text and/or graphics, which may alter content. The journal's standard [Terms & Conditions](#) and the [Ethical guidelines](#) still apply. In no event shall the Royal Society of Chemistry be held responsible for any errors or omissions in this *Accepted Manuscript* or any consequences arising from the use of any information it contains.

A Study of Procyanidin Binding to Histatin 5 using Electrospray Ionization Tandem Mass Spectrometry (ESI-MS/MS) and Molecular Simulations

Joshua Shraberg,^a Steven W. Rick,^{*a} Nalaka Rannulu,^a and Richard B. Cole^{*a,b}

Received Xth XXXXXXXXXXXX 20XX, Accepted Xth XXXXXXXXXXXX 20XX

First published on the web Xth XXXXXXXXXXXX 200X

DOI: 10.1039/b000000x

Tannins act as antioxidants, anticarcinogens, cardio-protectants, anti-inflammatory and anti-microbial agents and bind to salivary peptides by hydrophilic and hydrophobic mechanisms. Electrospray Ionization Mass Spectrometry (ESI-MS) has been used to assess both hydrophilic and hydrophobic components of noncovalent binding in protein complexes. In the present study, direct infusion Electrospray-Fourier Transform Ion Cyclotron Resonance Mass Spectrometry (ES-FTICR MS) is used to assess relative binding affinities of procyanidin tannin stereoisomers for salivary peptides arising from aqueous solutions. The condensed tannins procyanidin B1, B2, B3, and B4 demonstrate significantly different binding affinities for the salivary peptide Histatin 5. Rigid docking combined with molecular dynamics optimization is used to investigate procyanidin-Histatin 5 binding mechanisms and as a basis to rationalize trends found in the corresponding ES-FTICR MS experiments. The relative binding affinities of the four procyanidin rotamers are different in the gas and liquid phases. The simulation results indicate that many of the same contact points are made in both phases, but there is a decrease in strong electrostatic interactions and an increase in π - π contacts upon transfer from the gas to the liquid phase. The simulations reveal that the tannin interactions can make close contacts with a variety of amino acid residues on the peptide.

1 Introduction

Plant tannins are water-soluble polyphenolic compounds that have molecular weights ranging between 500 and 3000 Da.¹ In addition to participating in typical phenolic reactions, they possess unique properties such as the ability to precipitate alkaloids as well as proteins.² Tannins have generally been classified as either “hydrolyzable” (gallotannins and ellagitannins) or “condensed” based on their ability to readily undergo or resist hydrolysis.³

Tannins are present in a variety of plant foods in quantities up to several grams per kilogram.^{4,5} The intake of flavanoids (the class of polyphenols that includes condensed tannins) in the U.S. is estimated to be approximately 20 milligrams per day, though other estimates range up to 1 gram per day.^{4,6} Several varieties of tannins are suspected to produce hepatotoxicity, carcinogenesis, and anti-nutritional effects in animal studies.⁷ However, other studies indicate condensed tannins act as antioxidants, anticarcinogens, cardio-protectants, anti-inflammatory and antimicrobial agents. More investigation to determine the potential health benefits and adverse effects of

tannins as well as their mechanism(s) of action and bioavailability is therefore warranted.^{7,8}

Tannins bind and precipitate peptides with extended flexible conformations such as gelatin, though specificities of tannins for a particular peptide can vary considerably.^{9–12} Tannins bind salivary peptides even more strongly than gelatin, and are believed to be responsible for the sensation of astringency (dry sensation causing mouth puckering) associated with consumption of foods with high tannin content such as red wine and tea.⁴ In addition, condensed tannin-salivary peptide complexes remain relatively insoluble under conditions typically found in the digestive tract.^{13,14}

A significant portion of the salivary peptidome is generated through proteolysis of six classes of protein species secreted by the major salivary glands: acidic Proline Rich Proteins (aPRPs), basic Proline Rich Proteins (bPRPs), glycosylated Proline Rich Proteins (gPRPs), Histatins, Statherin, and Cystatins.^{15–17} PRPs constitute up to 70% of secreted salivary proteins and tannin binding is proposed to be the main function of bPRPs.^{16,18–23} Mass spectrometry has been successfully applied to the study of tannin-PRP interactions to determine the relative binding affinities and stoichiometries of various tannin-peptide complexes and to investigate the overall architecture of tannin-peptide complexes.^{24–26}

Human histatins belong to a family of antimicrobial pep-

^a Department of Chemistry, University of New Orleans, New Orleans, LA, 70148, US. Fax: 504-280-6860; Tel: 504-280-7412; E-mail: rcole@uno.edu

^b Université Pierre et Marie Curie (Paris 6), Institut Parisien de Chimie Moléculaire (UMR 8232), 4 Place Jussieu, 75252 Paris, France

tides that contain high numbers of histidines. Among the histatins, Histatin 5 in particular has been noted for antiviral activity, including inhibition of HIV-1 replication.²⁷ However, MS and NMR data regarding the strength of tannin-Histatin binding interactions appear somewhat contradictory.^{28–30} The Histatin 5 salivary peptide has been found to possess a +5 charge at neutral pH and an isoelectric point (pI) of 10.5 in aqueous solution.^{31,32} 2D NMR studies indicate Histatin 5 assumes a random coil in aqueous solution.^{33,34} Histatin 5 has a propensity to adopt transient helical conformations in DMSO, but a definitive global minimum energy conformation is lacking.³³ In addition, tertiary structural changes in Histatin 5 were not observed upon binding to the condensed tannin monomer epigallocatechin gallate (EGCG).²⁹

The condensed tannins procyanidin B1, B2, B3, and B4 are dimeric diastereomers of (+)-catechin and (-)-epicatechin units with structures: epicatechin-(4 β →8)-catechin, epicatechin-(4 β →8)-epicatechin, catechin-(4 α →8)-catechin, and catechin-(4 α →8)-epicatechin, respectively (Figure 1).⁷ These compounds were selected as model tannins to study binding interactions with Histatin 5 because they are found in many plants, and because they offer the possibility to probe the effect of subtle changes in procyanidin stereochemistry upon peptide binding strength. Each of the Procyanidins B1, B2, B3, and B4 adopt two distinct minimum energy conformations (rotamers) in aqueous solution corresponding to either a compact rotamer with π - π stacked monomers forming a dihedral angle at the interflavanoid bond (between C4 and C8) of +95°, or an extended unstacked rotamer with a dihedral angle of -81°.³⁵

Histatins possess a significantly different primary structure from other more abundant classes of salivary peptides (including a large percentage of histidine residues) and to our knowledge, studies of procyanidin binding to Histatin 5 have not been conducted. We used ES-FTICR MS to probe the relative binding affinities of procyanidin B1, B2, B3, and B4 for Histatin 5. The possibility for ESI-MS to measure relative binding affinities of tannin stereoisomers for various types of salivary peptides, including the antiviral Histatin 5, could permit the creation of a new tool for screening the bioavailability of tannins. Weaker binding tannins are predicted to be more susceptible to absorption from the gut and thus have higher bioavailability, though other factors including complexation with bile salts can influence the bioavailability of tannins.^{14,29,30} To rationalize procyanidin-Histatin 5 binding trends found in the ES-FTICR MS experiments, the compact and extended rotamers of procyanidin B1, B2, B3, and B4 were docked to Histatin 5 with FRED,^{37,38} and subsequently optimized in MD simulations using AMBER.³⁹

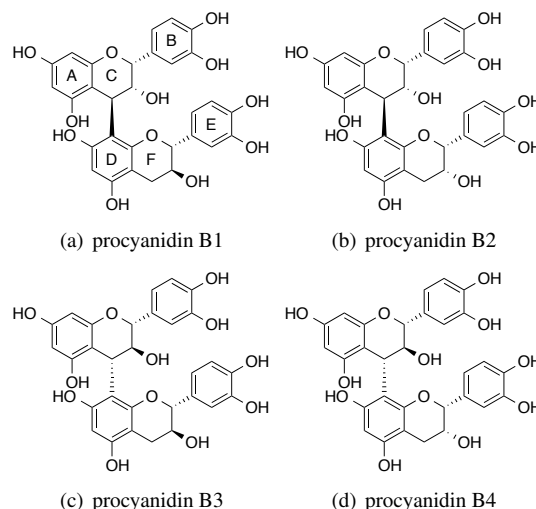


Fig. 1 Structures of dimeric procyanidin stereoisomers. Each dimer is composed of two subunits from either catechin or epicatechin monomers. The four stereoisomers are referred to as Procyanidin B1: epicatechin-(4 β →8)-catechin, Procyanidin B2: epicatechin-(4 β →8)-epicatechin, Procyanidin B3: catechin-(4 α →8)-catechin, and Procyanidin B4: catechin-(4 α →8)-epicatechin³⁶

2 Methods

2.1 Mass Spectrometry

All mass spectrometry experiments were performed in the positive ion mode on a Bruker (Billerica, MA) Apex Qe 7.0 T Fourier transform ion cyclotron resonance (FT-ICR) mass spectrometer equipped with an Apollo II ESI source. To obtain “soft” ionization conditions to allow conservation of noncovalent interactions between procyanidins and Histatin 5 while also maintaining strong signals, voltages on the capillary exit and the skimmer were set to -35 and -1.7 V, respectively. Positive ion direct infusion ESI-FTICR MS was used to evaluate the noncovalent binding of procyanidin B1, B2, B3, and B4 with the salivary peptide Histatin 5. Direct infusion ES-Qh-FTICR MS studies used a solution of 10 μ M Histatin 5 (DSHAKRHHGYKRFHEKHHSHRGY) and 40 μ M of procyanidin B1, B2, B3, or B4 in deionized water at pH of around 5.8. Note that this is slightly different than the pH of saliva, 6.8.⁴⁰ After mixing, the solution was kept at room temperature for 4 h before introducing the sample into the mass spectrometer. Data for the four stereoisomers were acquired under identical experimental conditions. Furthermore, it was found that refrigeration of the sample, or prolongation of the sitting time up to 24 h, did not significantly change signal intensities or binding ratios as compared to those observed

after four hours at room temperature. Notably, the appearance of signals corresponding to procyanidin-Histatin complexes could be observed by mass spectrometry even immediately upon mixing, but the intensities were low compared with longer waiting times. This supports the notion that the complex formation occurs in solution, rather than as a result of the ESI process.

The binding strength quotient, defined as the sum of the signals for all the different tannin-peptide complexes divided by the summed signals of unbound peptide,⁴¹ was calculated for each procyanidin-peptide mixture. Gas-phase dissociation quotients were also calculated for each procyanidin diastereomer by measuring the resistance of procyanidin-Histatin 5 complexes to collision-induced dissociation (CID) taking place in the hexapole collision cell at a collision energy of 10 eV. The dissociation quotient is defined as the sum of the product ion signals divided by the signal intensity of the parent ion. The four procyanidins have the same molecular weight, so the collision energies in the center-of-mass frame of reference will be identical for peptide complexes formed with each of the four procyanidins.

2.2 Simulations

Atomic coordinates for the compact and extended rotamers of procyanidin B1, B2, and B4, and the compact rotamer of procyanidin B3 were provided by Dr. Michel Laguerre of the Institut Européen de Chimie et de Biologie, Pessac, France. The extended rotamer of procyanidin B3 was obtained by rotation of the interflavanoid bond of the compact procyanidin B3 rotamer in PyMOL.⁴² The compact and extended structures of the four procyanidin molecules are given in Supplementary Information. Structural data for the Histatin 5 peptide is not available from a protein structure database. An initial structure for Histatin 5 was generated with CS23D2.0,⁴³ a web server for protein structure prediction from sequence data and NMR chemical shifts (Figure 2). Proton chemical shifts for Histatin 5 in 10 mM phosphate/H₂O buffer from a conformational study of Histatin 5 by Lajoie et al. were used as input for CS23D2.0.³³ CS23D2.0 was executed with the “number of GAFolder iterations” set to 100.

Simulations of the resulting structure were implemented with the *sander* module of AMBER 9³⁹ using the ff03 force field⁴⁴ with periodic boundary conditions. All bond lengths were constrained with the SHAKE algorithm and long-range electrostatics were treated with the particle mesh Ewald (PME) method. Partial charges for procyanidin atoms were fit to electrostatic potentials derived from closed-shell restricted Hartree-Fock calculations with the augmented cc-pVTZ basis set using the NWChem software package version 6.1.⁴⁵ Additional parameters for procyanidin atoms were obtained from gaff⁴⁶ atom parameters in the antechamber⁴⁷

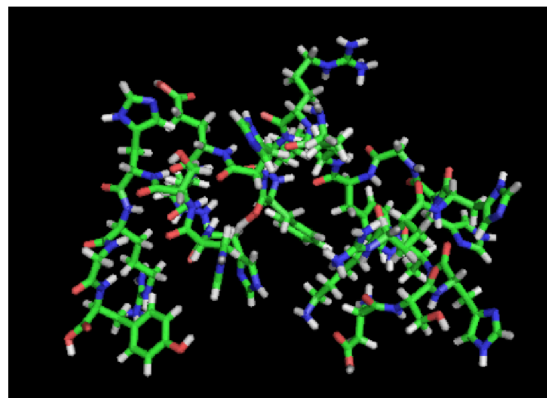


Fig. 2 Histatin 5 structure generated from CS23D2.0

module of AMBER. The Histatin 5 structure was neutralized by addition of 5 chloride ions and solvated in a box of 986 TIP3P⁴⁸ explicit waters. Fifty cycles of the steepest descent method followed by 50 cycles of conjugate gradient minimization were used with an 8 Å nonbonded cutoff to minimize the system. The system was equilibrated for 10 ps in MD simulations with a 9 Å nonbonded cutoff and a 1 fs time step under constant volume and temperature (NVT) conditions at 298 K using the weak coupling algorithm with a 0.5 ps time constant, followed by 140 ps of equilibration under constant temperature and pressure (NTP) conditions at 298 K and 1 bar. MD simulations were subsequently run under NTP conditions at 600 K for up to 0.5 ns, then cooled to 298 K at random time steps in order to obtain conformers potentially sampled by a Histatin 5 random coil. Six Histatin 5 conformers were selected for further analysis. All atom RMSDs between pairs of the six conformers ranged from 3.4 to 9.1 Å, while backbone RMSDs ranged from 2.0 to 8.3 Å. Scripts for processing MD trajectory data were written using Python 2.5.6 or Fortran 90 unless otherwise indicated.

The compact and extended rotamers of procyanidin B1, B2, B3, and B4 were docked to the six Histatin 5 conformers with FRED and optimized in both liquid-phase and gas-phase MD simulations with the *sander* module of AMBER (Figure 3). Receptor files were prepared in OEB format from the six Histatin 5 conformers with the FRED receptor GUI^{37,38} by extending a box around the volume of each conformer and the inner and outer contours were disabled. FRED was used with the default scoring function Chemgauss3 and the clash scale was set to 0.25 in order to avoid omission of relevant docking solutions due to an overly conservative clash scale. Liquid-phase MD optimization of procyanidins docked to Histatin 5 conformers was performed under periodic boundary conditions. Long-range electrostatics were handled with PME. Docked structures were neutralized by addition of 5 chlo-

ride ions and solvated in boxes of approximately 800 to 1100 TIP3P explicit water molecules. Each system was energy minimized with 50 cycles of the steepest descent method followed by 50 cycles of conjugate gradient minimization using a 12 Å nonbonded cutoff. Equilibration was performed for 10 ps with a 12 Å nonbonded cutoff and a 1 fs time step under NVT conditions at 298 K using Langevin dynamics temperature regulation with a collision frequency of 1 ps^{-1} , followed by 160 ps of equilibration under NTP conditions at 298 K and 1 bar. MD simulations were subsequently run under NTP conditions at 298 K for 1 ns. Liquid-phase simulations of unbound compact and extended rotamers of procyanidin B1, B2, B3, and B4 were run for 1 ns at 298 K using a similar method. No conformational changes were observed between compact and extended forms in liquid-phase simulations of bound and unbound procyanidins.

In the ESI-MS studies, the strongest peaks observed for procyanidin-Histatin 5 complexes had a 1:1 binding stoichiometry and a net charge of +5. In addition, the charge state distribution of procyanidin-Histatin 5 complexes was the same as for the unbound peptide. Thus, it is assumed Histatin 5 possesses all the charge (present as excess protons) contained in the complexes, while procyanidins bind as neutrals. Gas-phase MD optimization of procyanidins docked to Histatin 5 conformers was performed *in vacuo* with periodic boundary conditions disabled and all electrostatic interactions calculated directly. Docked structures were not neutralized by the addition of ions in order to simulate the +5 net charge of procyanidin-Histatin 5 complexes in the ESI-MS experiments. Each system was energy minimized with 50 cycles of the steepest descent method followed by 50 cycles of conjugate gradient minimization using a nonbonded cutoff of 999 Å. The systems were equilibrated for 170 ps with a 999 Å nonbonded cutoff at a constant temperature of 298 K using Langevin dynamics temperature regulation with a collision frequency of 1 ps^{-1} . The temperature was increased from 298 K to 448 K during an additional 100 ps of equilibration as done in previous studies to simulate typical conditions in ESI-MS experiments.^{49–53} MD simulations were subsequently run under constant temperature conditions at 448 K for 1 ns. Gas-phase simulations of unbound compact and extended rotamers of procyanidin B1, B2, B3, and B4 were run for 1 ns at 448 K using a similar method. No conformational changes were observed between compact and extended forms in the gas-phase simulations of bound and unbound procyanidins.

3 Results

3.1 ESI-MS Analysis

When subjected to direct infusion in the absence of procyanidins, Histatin 5 (10 μM in de-ionized water) exhibited a se-

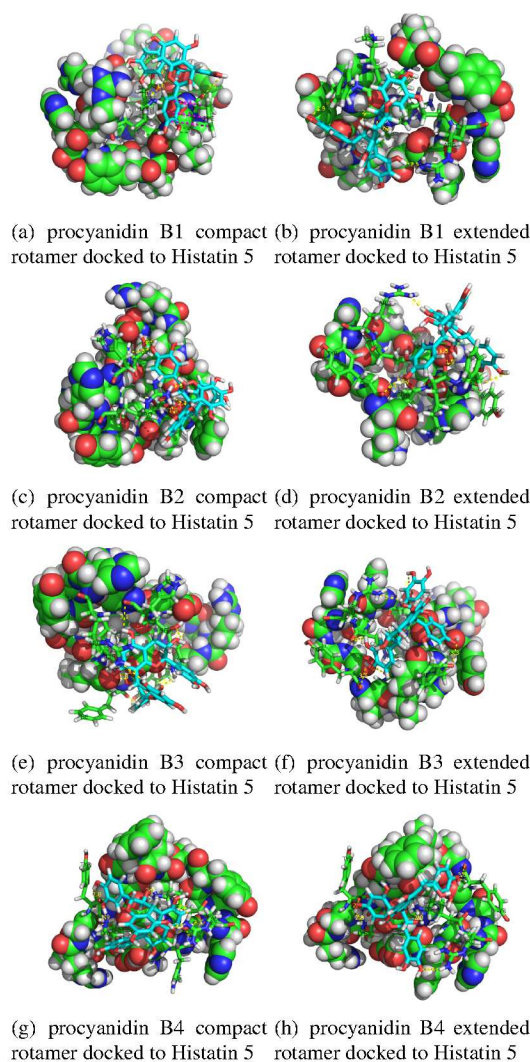


Fig. 3 Interatomic distances of hydrogen bond forming atoms (dashed yellow lines) and π - π stacking atoms (dashed magenta lines) of compact and extended rotamers of procyanidin B1, B2, B3, and B4 docked to a Histatin 5 conformer

ries of peaks corresponding to multiply charged ions ranging from +4 to +8. Although the initial solution conditions can give an indication of the initial peptide charge in solution (e.g., a charge state of +5 at pH 7³²), a complex series of events takes place leading up to desorption of species into the gas phase during the ESI process. The result is that a distribution of charge states will be observed in the ESI mass spectrum. This gas-phase distribution will often not reflect the charge state(s) of species in the initial neutral solution.^{54,55} At the employed Histatin 5 : procyanidin molar ratio of 1:4, a variety of peaks corresponding to noncovalent complexes of multiply charged [Histatin 5 + procyanidin] aggregates were observed.

The charge state distribution of these complexes exactly mirrored that of the unbound peptide (i.e., +4 to +8). This range of charge state distribution, as well as the observed range of stoichiometry ratios between noncovalently binding Histatin 5 and procyanidin (as many as five procyanidin molecules per Histatin 5, but never more than one Histatin 5 binding to a single procyanidin molecule), were the same for all four procyanidin isomers. A representative ESI mass spectrum is shown in Figure 4 for procyanidin B2.

It should be noted that epigallocatechin-3-gallate (EGCG), a polyphenol with a structure closely related to those of the procyanidins has been shown to be capable of forming covalent linkages with cysteine-containing peptides via reaction of the nucleophilic thiol group of cysteine.^{56–58} No such thiol group is present on Histatin 5, which rules out the possibility for this type of reaction in our tannin-peptide system. Moreover, another study concurs that thiol groups are the peptide sites that are most reactive with ECGC, but also states that the formation of covalently bound Schiff base adducts is possible from N-termini amino groups, or to a lesser extent, from primary amino sites on arginine residues contained in peptides.⁵⁹ The authors speculate that an ECGC-quinone was formed as an (oxidized) intermediate that reacted with the primary amine nucleophiles, but such Schiff base formation requires a free amino group to initiate the reaction. Because our solutions were prepared at pH 5.8, the possibility that primary amines were not protonated is minimized; we are thereby fully confident that covalent bond formation was not a factor in our analysis, and that the observed [Histatin 5 + procyanidin] complexes represent noncovalently bound species.

Binding strength quotients were calculated for each tannin-peptide mixture.⁴¹ The resulting data are compiled in Table 1. Statistical analysis (t-test) showed a statistically significant difference between the binding strength quotients obtained for each of these procyanidin isomers. The relative binding affinities of the four procyanidin diastereomers in solution were ranked according to their corresponding binding strength quotients: B1 > B4 > B2 > B3.

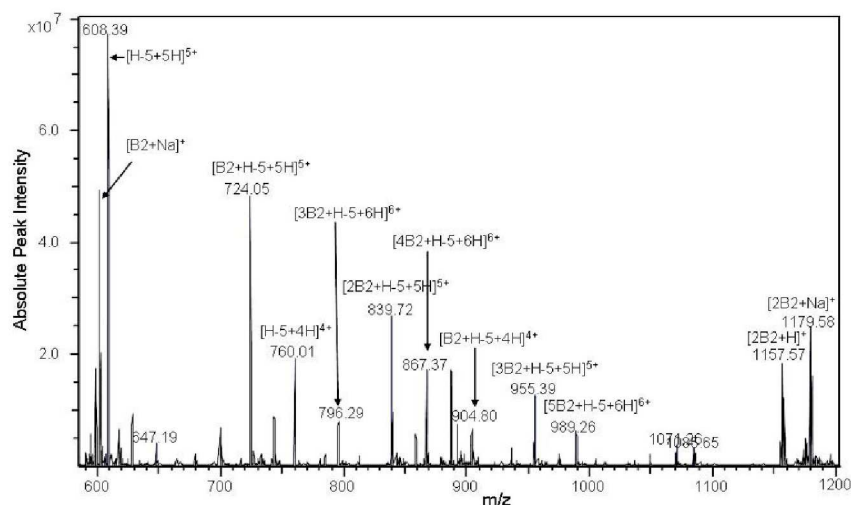


Fig. 4 Positive ion ES-FTICR mass spectrum of 4:1 [B2:H-5] in pure water, establishing the ability to observe intact complexes of a representative dimeric procyanidin (B2) with the salivary peptide Histatin 5 (H-5). Peaks at m/z 724.1 and 904.8 correspond to 1:1 [B2:H-5] complexes of +5 and +4 charge state, respectively. The peak at m/z 839.7 corresponds to the 2:1 complex of +5 charge state. Peaks at m/z 796.3 and 955.4 correspond to 3:1 complexes of +6 and +5 charge state, respectively. The peak at m/z 989.3 corresponds to a 5:1 complex of +6 charge state, whereas the peak at m/z 867.4 corresponds to a 4:1 complex of +6 charge state. Complexes were detected at the same charge states as those obtained separately for the free peptide, suggesting that procyanidin molecules bind to the peptides as neutrals. Although Histatin 5 binds readily with more than one procyanidin molecule for all procyanidin isomers, binding of multiple peptide molecules to one molecule of procyanidin was not observed.

Table 1 ESI-MS binding strength quotients (averaged over 4 to 7 trials) of procyanidin B1, B2, B3 and B4 (PCB: Procyanidin B)

PCB	Binding strength quotient	Rank
PCB1	0.36 ± 0.01	1
PCB4	0.32 ± 0.02	2
PCB2	0.27 ± 0.03	3
PCB3	0.210 ± 0.004	4
PCB	Gas-phase dissociation quotient	Rank
PCB4	1.4 ± 0.2	1
PCB2	4.1 ± 0.5	2
PCB1	8 ± 3	3
PCB3	14 ± 3	4

Subsequent tandem mass spectrometry experiments were performed to determine the relative strengths of tannin-peptide complexes in the gas phase for all four procyanidin diastereomers. Mass-selected precursors corresponding to (B + H-5 + 5H⁺) ions at *m/z* 724.1 for each of the four procyanidins were subjected to collision induced decomposition (CID). This (B + H-5 + 5H⁺) peak was very strong and stable for all four procyanidins, and all four diastereomers exhibited both B and H-5 ions in CID product ion spectra. Gas-phase dissociation quotients were obtained at a collision gas energy of 10 eV using argon as collision gas. Results show that (B + H-5 + 5H⁺) (*m/z* 724.1) complexes resist dissociation in the order: B4 > B2 > B1 > B3 in the gas phase (Table 1). This order is thus indicative of the relative binding affinities of procyanidin diastereomers to Histatin-5 in the gas phase.

The four procyanidins thus exhibit different relative rankings according to the gas-phase dissociation quotients as compared to the ESI-MS binding strength quotients. This is not entirely surprising, because the two parameters do not measure precisely the same phenomena. The gas-phase dissociation quotient ranking reflects the relative tendency for a gas-phase tannin-protein complex to dissociate under collision with a neutral gas. One starts by selecting a gas-phase complex and the yield of gas-phase products appearing at the exit of the collision cell is measured; thus, only gas-phase entities are considered. This differs from the ESI-MS binding strength quotient which indicates the tendency for tannin-peptide complexes to form (as opposed to remaining unbound) from solutions containing the two entities that are undergoing electrospray. Here, the peptide and tannin have the opportunity to make initial contact in solution, then they are desorbed into the gas-phase as solvated entities which undergo desolvation before detection by the mass spectrometer. The ESI-MS binding strength quotient thus gauges the tendency for tannin-peptide complexes to form and survive the transition from the solution phase to the gas phase.

3.2 Simulation Analysis of Procyanidin-Histatin 5 Complexes

3.2.1 Analysis of Compact Versus Extended Procyanidin Rotamer Stability.

The two separated procyanidin rotamers, compact and open,³⁵ do not interconvert on the time scale of the simulations. All simulations were done for both conformations. To determine which conformation corresponds to the stable conformation, either when bound or free and in the gas and liquid phase, the intramolecular or self energy was calculated. The self energy is the sum of the Lennard-Jones and Coulombic interactions between atoms on the same molecule, the angle and the torsional energy terms. The compact rotamers of unbound procyanidin B2 and B3 exhibit lower energies than the extended rotamers in the gas phase, while the extended rotamers of procyanidins B1 and B4 have a lower energy than the compact rotamer (Table 2). These energy differences are from 16 kcal/mol to 43 kcal/mol and so represent a significant amount of energy. This implies that in the gas phase B1 and B4 are extended and the others are compact. In the liquid phase, this analysis is complicated by interactions with the solvent. NMR experiments indicate that all four tannin molecules exist in both conformations in solution.³⁵ Strain induced by binding of procyanidin rotamers to Histatin 5 was quantified as the difference between the self energies of bound and unbound procyanidin diastereomers. This definition of strain energy would include both the loss of hydrogen bonds and other favorable intramolecular interactions as well as an increase in torsional and bond angle energies. The strain energies are small, approximately 10 kcal/mol or less, for both rotamers in the gas and liquid-phases (Table 3), which suggests that there is little structural rearrangement of the molecule as it binds the peptide.

Table 2 Average unbound gas-phase procyanidin rotamer self energies in the compact and extended forms, in kcal/mol.

	Gas-phase procyanidin-Histatin 5 self energies	
	Compact	Extended
PCB1	-679 ± 9	-702 ± 9
PCB2	-578 ± 9	-562 ± 9
PCB3	-454 ± 9	-411 ± 9
PCB4	-388 ± 9	-422 ± 9

3.2.2 Procyanidin-Histatin 5 Interaction Energy Analysis.

Following liquid and gas-phase optimization of procyanidin diastereomers in complex with the six Histatin 5 conformers, procyanidin-Histatin 5 interaction energies were calculated based on their direct interaction energies, and averaged over the 1 ns trajectories. The energy of binding can be separated into a number of different components, including

Table 3 Average rotamer strain energies, in kcal/mol.

Liquid-phase procyanidin-Histatin 5 strain energies		
	Compact	Extended
PCB1	-3 ± 7	13 ± 8
PCB2	2 ± 2	0 ± 7
PCB3	2 ± 6	3 ± 6
PCB4	1 ± 6	-1 ± 6
Gas-phase procyanidin-Histatin 5 strain energies		
PCB1	0 ± 10	10 ± 20
PCB2	2 ± 9	4 ± 8
PCB3	7 ± 8	14 ± 10
PCB4	11 ± 8	4 ± 9

direct procyanidin-Histatin 5 interactions, changes in the procyanidin and Histatin 5 intramolecular interactions, and loss of solvent interactions (for liquid-phase binding). We can use the direct interactions as an indication of the binding energies. The interaction energies are given in Table 4, for the compact and extended rotamer as well as the average of the two. The liquid-phase interaction energies are less than the gas phase values, suggesting there are less direct strong ligand-peptide interactions. Some interactions may be solvent mediated, with bridging water molecules. From the data in Tables 2 and 4, some conclusions about which rotamer is more stable in the bound and unbound state and about the ranking of the procyanidin binding affinities can be made.

Table 4 Average procyanidin-Histatin 5 interaction energies of procyanidin B1, B2, B3, and B4 in the liquid and gas phase, comparing the values for the compact, extended and the average of the two rotamers, in kcal/mol.

Liquid-phase procyanidin-Histatin 5 interaction energies			
	Compact	Extended	Average
PCB1	-49.3 ± 0.3	-59.5 ± 0.2	-54.4 ± 0.2
PCB2	-52.2 ± 0.3	-52.0 ± 0.3	-52.1 ± 0.2
PCB3	-40.0 ± 0.2	-55.9 ± 0.3	-48.0 ± 0.2
PCB4	-54.5 ± 0.4	-50.6 ± 0.3	-52.5 ± 0.2
Gas-phase procyanidin-Histatin 5 interaction energies			
PCB1	-76.4 ± 0.2	-89.1 ± 0.2	-82.8 ± 0.2
PCB2	-84.1 ± 0.3	-88.8 ± 0.2	-86.4 ± 0.2
PCB3	-78.6 ± 0.3	-87.6 ± 0.3	-83.1 ± 0.2
PCB4	-82.2 ± 0.3	-89.9 ± 0.3	-86.1 ± 0.2

The gas-phase binding will be considered first. The molecules B1 and B4 are more stable in the extended form when unbound, in the gas phase. Upon binding they can either remain in the same rotamer state or change. In the gas phase, the interaction energy for B1 is 13 kcal/mol more fa-

vorable in the extended form, so that tannin would be expected to stay in the extended form. For B4, the interaction energy is 8 kcal/mol more favorable in the extended form, so that tannin would also be expected to stay in the extended form. Both B1 and B4 would be predicted to stay in the extended form upon binding. The molecules B2 and B3 are most stable, when unbound, as compact. For both of these tannins, there is not a big enough gain in interaction energy for the extended form to compensate for the self energy increase. That would suggest that both B2 and B3 also do not change rotamer state upon binding.

Taking the interaction energies of the most stable rotamer (extended for B1 and B4 and compact for B2 and B3) as an estimate of binding affinities, we can get the following rankings: B4 > B1 > B2 > B3 in the gas phase. This gives reasonable agreement with the gas-phase data from Table 1 (B4 > B2 > B1 > B3). The interaction energies for the extended rotamer are all very close and what separates the affinity is that B2 and B3 bind as compact rotamers. It is worth emphasizing that our computational rankings are not based on free energies of binding and so are approximate estimates. In addition our experimentally-determined gas-phase binding affinities from ESI-MS/MS are not only indicative of binding free energies but of barriers to dissociate. In addition, the MS data includes not only the 1:1 complex, as treated in the simulations, but up to the 5:1 tannin:Histatin complex. The presence of other ligands may change the relative binding affinities. The calculated interactions energies do not vary by more than 10 kcal/mol among the different procyanidin molecules, while the ESI-MS dissociation constants vary by a factor of 10. This suggests that the large difference in binding affinities seen experimentally is not due to the direct interactions, but other factors, such as entropy.

For the liquid phase, the self-energy alone cannot be used to predict the relative stabilities of the rotamers. Assuming both forms are present in solution as indicated by experiment³⁵ and using the average for both rotamers from Table 4 gives this ranking: B1 > B4 > B2 > B3, which, perhaps fortuitously, agrees exactly with experimental rankings obtained using the ESI-MS binding strength quotients (Table 1). The liquid phase ESI-MS binding strength quotients are relatively close to each other and do not show the wide spread that the gas phase data showed. The computed interaction energies also do not show much of variation.

3.2.3 Analysis of Simulated Structures. The percentage of nearest neighbor atom contacts within a distance of 4 Å between procyanidin diastereomers and each residue of Histatin 5 was calculated by averaging the number of contacts over the 1 ns trajectories (Figure 5). Since a ligand can be in contact with more than one residue at a time, the percentages from Figure 5 do not have to sum to 100%. More nearest

neighbor contacts were observed in gas versus liquid-phase procyanidin-Histatin 5 complexes, suggesting that in the liquid phase, some interactions are solvent mediated, as mentioned previously. In addition, the relative number of contacts of each residue in the procyanidin-Histatin 5 complexes resembled average changes in the proton chemical shifts of Histatin 5 residues upon titration with EGCG as determined in 2D NMR studies by Bennick et al.²⁹ Structures of the procyanidin-Histatin 5 complexes corresponding to the maxima were inspected visually to determine the binding characteristics of potential procyanidin-Histatin 5 binding modes (data not shown). Procyanidin B1, B2, B3, and B4 bound multiple sites on Histatin 5 in multiple ligand conformations in both the gas and liquid phase. Gas-phase binding modes mostly exhibited structural characteristics representative of hydrogen bonding interactions. However, gas-phase binding modes also exhibited π - π stacking orientations and interatomic distances approximating the sum of van der Waals radii between procyanidin polyphenol rings and phenylalanine, tyrosine, and histidine rings of Histatin 5. The majority of liquid-phase binding modes exhibited hydrogen bonding and π - π stacking characteristics.

The percentage of intermolecular π - π stacking interactions in procyanidin-Histatin 5 complexes was assessed by averaging the number of intermolecular carbon-carbon or carbon-nitrogen contacts less than 4.0 Å between procyanidin polyphenol rings and aromatic side chain atoms of Histatin 5 over the 1 ns trajectories, and by visual inspection for π - π stacking orientations between the procyanidin polyphenol rings and aromatic side chains of Histatin 5. The criteria for π - π stacking between procyanidins and Histatin 5 were: intermolecular carbon-carbon or carbon-nitrogen contacts less than 4.0 Å and parallel planar orientations between procyanidin polyphenol rings and the aromatic side chains of phenylalanine, tyrosine, or histidine. To compare π - π stacking in liquid versus gas-phase procyanidin-Histatin 5 complexes, the average percentage of π - π stacking of each procyanidin diastereomer for the six Histatin 5 conformers was calculated. The average percentage of carbon-carbon and carbon-nitrogen contacts was greater in liquid versus gas-phase procyanidin-Histatin 5 complexes, though the relative number of carbon-carbon and carbon-nitrogen contacts for aromatic residues in the gas and liquid phase were similar (Figure 6). In addition, both liquid and gas-phase procyanidin-Histatin 5 complexes exhibited parallel planar orientations between the procyanidin polyphenol rings and aromatic side chains of phenylalanine, tyrosine, and histidine (Figure 7).

Intermolecular hydrogen bonding between procyanidin rotamers and a Histatin 5 conformer was assessed using a donor-acceptor cutoff distance of 3.2 Å and a 20° cutoff angle. A greater number of Histatin 5 residues participated in hydrogen bonding in gas-phase versus liquid-phase procyanidin-

Table 5 Percentage of intermolecular hydrogen bonding in gas and liquid-phase procyanidin-Histatin 5 complexes (PCB1: procyanidin B1, Side: Side Chain Atom, Main: Main Chain Atom)⁶⁰

(a) gas-phase compact rotamer of procyanidin B1 and a Histatin 5 conformer

donor	acceptor	hydrogen bonds
TYR10-Side	PCB1-Side	2.5%
LYS13-Side	PCB1-Side	19.6%
PCB1-Side	HID15-Side	15.3%
HID15-Side	PCB1-Side	2.1%
HIE19-Side	PCB1-Side	3.1%
PCB1-Side	TYR24-Side	0.1%
PCB1-Side	PHE14-Main	7.3%
HIE18-Side	PCB1-Side	5.7%
PCB1-Side	HIE19-Side	3.8%
PCB1-Side	TYR10-Side	1%
PCB1-Side	LYS13-Main	6.4%
TYR24-Side	PCB1-Side	0.4%
PCB1-Side	SER20-Side	0.1%
ARG22-Side	PCB1-Side	0.9%
PCB1-Side	HIE18-Main	0.5%

(b) liquid-phase compact rotamer of procyanidin B1 and a Histatin 5 conformer

donor	acceptor	hydrogen bonds
PCB1-Side	PHE14-Main	42.5%
LYS5-Side	PCB1-Side	1.8%
PCB1-Side	ALA4-Main	0.4%
LYS17-Side	PCB1-Side	0.1%
HID15-Side	PCB1-Side	1.3%
PCB1-Side	HIE18-Side	0.2%

(c) gas-phase extended rotamer of procyanidin B1 and a Histatin 5 conformer

donor	acceptor	hydrogen bonds
PCB1-Side	HID15-Side	1.3%
ARG6-Side	PCB1-Side	4.9%
ASP1-Main	PCB1-Side	21.3%
LYS5-Side	PCB1-Side	14.5%
PCB1-Side	TYR10-Side	0.1%
PCB1-Side	ASP1-Side	56.7%
TYR10-Side	PCB1-Side	0.6%
PCB1-Side	PHE14-Main	1.1%
SER2-Side	PCB1-Side	29.6%
SER2-Main	PCB1-Side	13.5%
PCB1-Side	SER2-Side	2.1%

(d) liquid-phase extended rotamer of procyanidin B1 and a Histatin 5 conformer

donor	acceptor	hydrogen bonds
PCB1-Side	PHE14-Main	6.9%
LYS13-Side	PCB1-Side	1.7%
LYS5-Side	PCB1-Side	3.6%
ARG22-Side	PCB1-Side	1.2%
TYR10-Side	PCB1-Side	0.9%

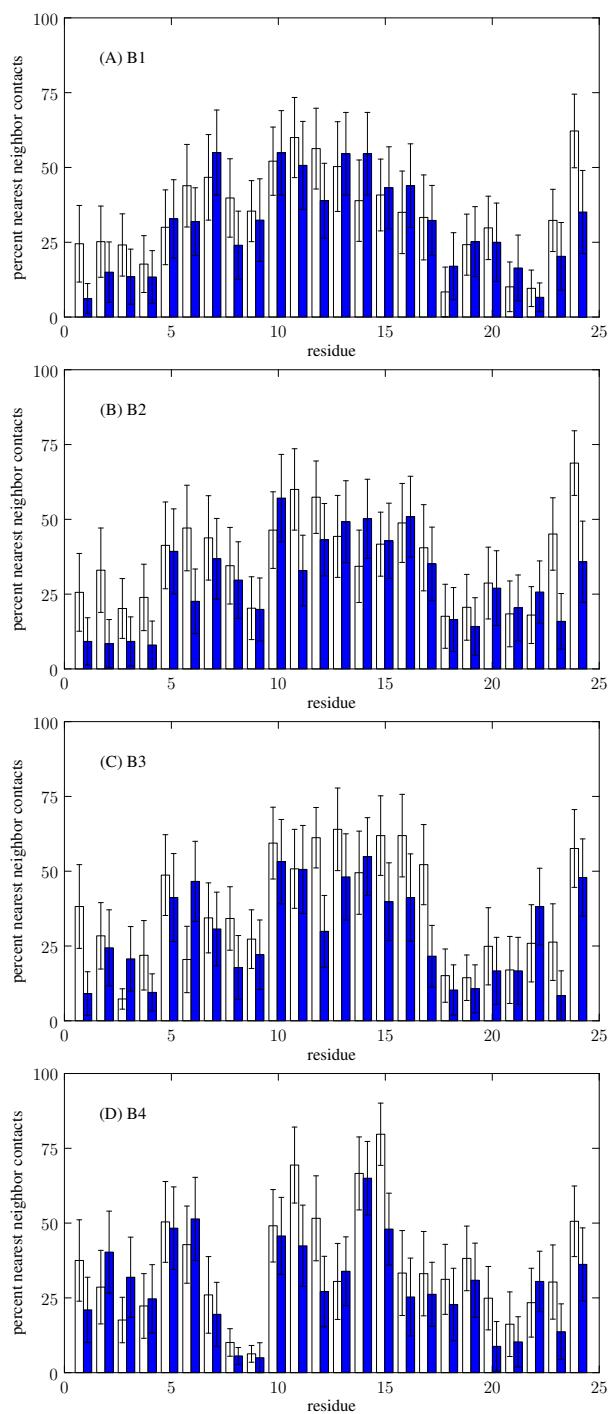


Fig. 5 Average percentage of nearest neighbor contacts less than 4 Å of procyanidins for the four procyanidin molecules in the gas (empty) and liquid (blue) phases.

Histatin 5 complexes (Table 5). In addition, the percentage of hydrogen bonding during the 1 ns trajectories was greater

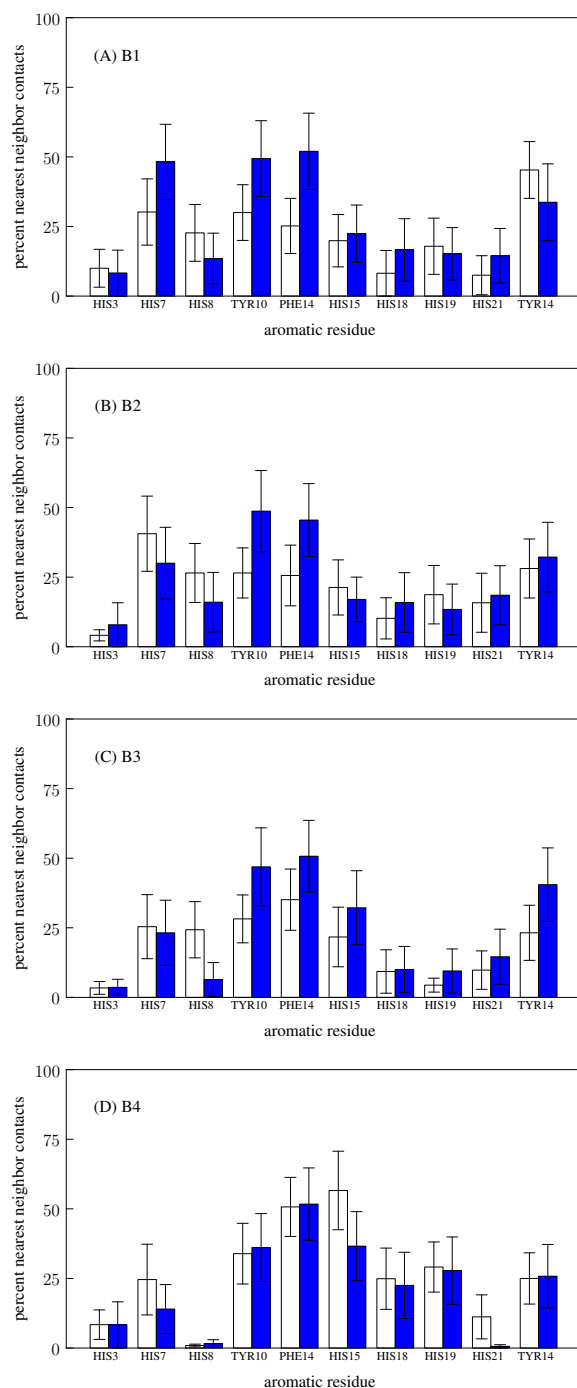
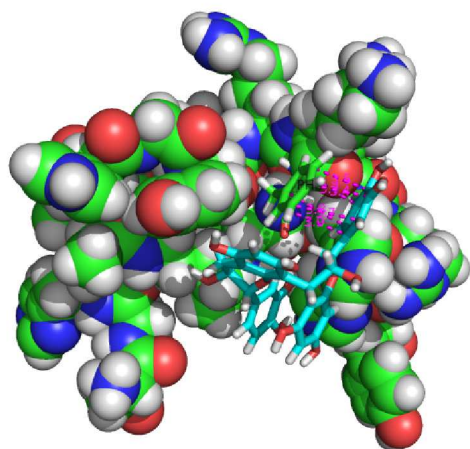
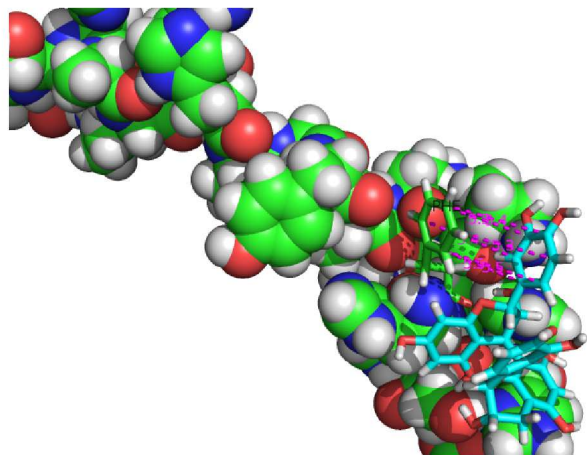


Fig. 6 Average percentage of carbon-carbon and carbon-nitrogen contacts less than 4 Å of procyanidins for 6 conformers of Histatin 5 in the gas (empty) and liquid (blue) phases.

for gas versus liquid-phase procyanidin rotamers (Table 5).



(a) π - π stacking between the compact rotamer of procyanidin B1 and phenylalanine 14 of Histatin 5 during liquid-phase optimization



(b) π - π stacking between the compact rotamer of procyanidin B1 and phenylalanine 14 of Histatin 5 during gas-phase optimization

Fig. 7 Intermolecular π - π stacking (dashed magenta lines) between a polyphenol ring of the compact rotamer of procyanidin B1 and phenylalanine 14 of a Histatin 5 conformer during liquid and gas-phase simulations

4 Discussion

Tannin binding to salivary peptides is attributed to both hydrophilic and hydrophobic mechanisms.^{61,62} Predominantly hydrophilic binding interactions have been proposed for condensed tannins through hydrogen bonding of their phenolic hydroxyl groups, whereas hydrolyzable tannins have been suggested to bind via mostly hydrophobic interactions through π - π stacking of their phenolic rings.⁶³ However, condensed tannins were found to bind proline rings of PRPs via π - π stacking of their polyphenol rings, and the relative binding affinities of a selection of tannins, including both hydrolyzable tannins and condensed tannin monomers, corresponded to the number of aromatic rings available for π - π stacking.^{29,30,64} In addition, the binding mechanism for the condensed tannin diastereomers procyanidin B1, B2, B3, and B4 to the 14 residue PRP IB7₁₄ was found to depend on the concentration of procyanidins, with hydrophilic interactions occurring at concentrations below the critical micelle concentration (CMC), while above the CMC, both hydrophilic and hydrophobic interactions were observed.^{65,66}

Association constants for self-aggregation of procyanidin diastereomers were measured to be around 6 M^{-1} .⁶⁷ 2D NMR studies of procyanidin binding to IB7₁₄ were performed below their self association constants, though self-aggregation was taken into account when calculating procyanidin-IB7₁₄ dissociation constants.^{65,66} The procyanidin-IB7₁₄ binding studies used 1 mM peptide and 1 to 7 mM of procyanidins in 12% ethanol and 5 mM acetic acid at pH 3.5.⁶⁶ CMCs for procyanidin B1, B2, B3, and B4 range from 19 to 28 mM.⁶⁷ Procyanidin-IB7₁₄ binding studies demonstrated that the tendency for procyanidin diastereomers to adopt the extended versus compact rotamer determined their relative binding affinities for IB7₁₄ in aqueous solution.^{65,66} Below the CMC and at a tannin:peptide molar ratio > 2 , the tendency for procyanidin diastereomers to adopt the extended rotamer correlated with the amount of IB7₁₄ peptide precipitated. Above the CMC, the conformational preference of procyanidins did not influence their binding to IB7₁₄ due to the effects of tannin aggregation. Procyanidin B2 had the highest percentage of extended rotamer (45%), followed by B4(17%), B1(8%), and B3(5%).³⁵ Below the CMC, the dissociation constants of procyanidin B1, B2, B3, and B4 for IB7₁₄ were calculated to be 2.9 mM, 1.1 mM, 8.0 mM, and 2.5 mM, respectively, and the number of IB7₁₄ binding sites for procyanidin B1, B2, B3, and B4 were found to be 3.0, 3.2, 3.0, and 3.5, respectively. Thus, the relative binding affinities of the procyanidin diastereomers for IB7₁₄ were ranked: B2 $>$ B4 $>$ B1 $>$ B3. In our study, both compact and extended rotamers of procyanidin B1, B2, B3, and B4 were docked to the six Histatin 5 conformers with FRED to adequately sample the most significant conformations contributing to procyanidin binding to Histatin 5.

2D NMR studies have shown that Histatin 5 adopts a random coil in aqueous solution.^{33,34} Intrinsically unstructured proteins (IUPs) include random coil, molten globule (containing secondary structure, but without compact tertiary structure), and their transitions along with transitions to the folded state.⁶⁸ IUPs have often been found to be characterized by a high net charge and/or a large number of polar amino acids.^{69,70} Histatin 5 shares many of the features of IUPs, including a net charge of +5 in neutral aqueous solution as well as a large number of polar and aromatic residues, including histidine, tyrosine, phenylalanine, lysine, and arginine.³² Bennick et al.²⁹ determined that the relative number of nearest neighbor contacts between Histatin 5 residues and procyanidin diastereomers could be assessed by monitoring average changes in proton chemical shifts of Histatin 5 residues upon titration with EGCG. A larger number of contacts corresponded to a larger average chemical shift change. The average chemical shift changes are suggested to be due to hydrophobic interactions between aromatic rings of EGCG and aromatic side chains of histidine, phenylalanine, and tyrosine, and also hydrophobic sections of the side chains of lysine and arginine. A significant number of contacts were observed for histidine, tyrosine, and phenylalanine, and also arginine and lysine during simulations of the procyanidin-Histatin 5 complexes. These simulation data suggest procyanidins may bind a diverse array of peptide backbone conformations sampled by a Histatin 5 random coil in aqueous solution via mostly hydrophobic and π - π stacking interactions between procyanidin polyphenol rings and histidine, phenylalanine, tyrosine, lysine, or arginine residues of Histatin 5. In contrast, a mixture of tannin-peptide complexes resulting from tertiary structural changes was observed upon binding of EGCG to the 70 residue proline-rich IB-5.²⁶ Future studies of conformational changes in Histatin 5 upon binding procyanidins using NMR with residual dipolar couplings (RDC) and conformations of bound procyanidins using time-averaged Nuclear Overhauser Effect (NOE) could serve to further elucidate the mechanisms of procyanidin-Histatin 5 binding in aqueous solution.⁷¹⁻⁷³ 2D NMR studies showed that the primary sequence of Histatin 5 can affect tannin binding as well, perhaps due to some element of binding cooperativity, though this effect was not investigated in the current study.^{29,74}

5 Conclusions

Estimates of the binding affinity from calculating the direct interaction energy between the procyanidin and Histatin 5 gave a ranking for the four diastereomers in good agreement with the ESI-MS for both the gas and the liquid phases. The procyanidin-Histatin 5 interactions are different between the gas and the liquid phase in three separate ways. First, the number of Histatin 5 residues involved in hydrogen bonding

was greater for gas versus liquid-phase procyanidin-Histatin 5 complexes (Table 5). The percentage of hydrogen bonding during the MD simulations was also greater for gas versus liquid-phase complexes. Secondly, in the liquid phase the percentage of intermolecular π - π stacking interactions between the procyanidins and Histatin 5 is enhanced (Figure 6). And finally, the average procyanidin-Histatin 5 binding energies in gas-phase procyanidin-Histatin 5 complexes were around 30 kcal/mol lower than in the liquid phase. Together these three effects (more hydrogen bonding in the gas-phase, more π - π stacking in the liquid phase, and stronger interactions overall in the gas phase) indicate that the structures of the complexes are influenced by water, which is consistent with the different ranking of binding strengths that were measured (Table 1). Enhanced electrostatic interactions in the gas-phase procyanidin-Histatin 5 complexes were seen in other studies (Table 4).^{24,25}

NMR studies employing time-averaged NOEs demonstrated that multiple conformations of EGCG bound several sites of a PRP heptapeptide.⁷³ Visual inspection of structures corresponding to maxima in the energy distributions of procyanidin-Histatin 5 complexes suggests that the compact and extended conformations of procyanidin B1, B2, B3, and B4 bind multiple sites on Histatin 5 as well (data not shown). In addition, both gas and liquid-phase binding modes of procyanidin-Histatin 5 complexes exhibited hydrogen bonding and π - π stacking characteristics, though gas-phase binding modes appeared to exhibit more hydrogen bonding and less π - π stacking than liquid-phase binding modes, as expected (data not shown).

It is estimated that 25% of the total protein in mammals consists of IUPs and efficient methods for predicting IUPs are currently being developed.^{75–80} Intrinsic disorder can provide a receptor with additional functional properties compared with the folded state, including broader specificity to interact with a wider variety of ligands as well as the ability to interact with more ligands simultaneously.^{81–83} The protein structure-function paradigm can thus be modified to encompass IUPs by including random coil, molten globule (containing secondary structure, but without compact tertiary structure), and folded states, along with their transitions.⁶⁸ From an evolutionary standpoint, it would appear energetically costly to have to synthesize and process a large number of folded proteins capable of binding each species of tannin. Thus, it seems appropriate that intrinsic disorder imparts salivary peptides with the ability to bind a greater variety of tannins than the folded state.⁸⁴ However, the energetic cost of broader specificity imparted to a peptide by intrinsic disorder may result in lower tannin binding affinities overall.^{68,85} Tannins that do not bind strongly to salivary peptides would be expected to be more bioavailable, and could potentially be exploited for their antioxidant potential.²⁹ Mass spectrometry, with its rapid and sensitive screen-

ing ability, may be particularly well suited for determining the bioavailability of tannins.^{24,25,86,87}

Acknowledgement. We would like to thank Richard W. Hemingway and Dr. H el ene Fulcrand for helpful discussions. We would also like to acknowledge Dr. Michel Laguerre, Dr. Anders Bennick, Dr. Michael P. Williamson, and Dr. James Gumbart for their valuable discussion and assistance. This work was supported by the National Science Foundation (NSF) under Contract No. CHE-1058764.

References

- 1 K. Khanbabaee and T. van Ree, *Nat. Prod. Rep.*, 2001, **18**, 641–649.
- 2 T. Swain and E. Bate-Smith in *Comparative Biochemistry*, ed. M. Florin and H. Mason; Academic Press, New York and London, 1962; p. 764.
- 3 D. Griffiths in *Toxic Substances in Crop Plants*, ed. J. P. F. D’Mello, C. M. Duffus, and J. H. Duffus; The Royal Society of Chemistry, Cambridge, 1991; pp. 180–181.
- 4 A. Bennick, *Critical Reviews in Oral Biology & Medicine*, 2002, **13**, 184–196.
- 5 H. Mehansho, L. G. Butler, and D. M. Carlson, *Ann. Rev. Nutr.*, 1987, **7**, 423–440.
- 6 G. R. Beecher, *J. Nutr.*, 2003, **133**, 3248S–3254S.
- 7 V. Koleckar, K. Kubikova, Z. Rehakova, K. Kuca, D. Jun, L. Jahodar, and L. Opletal, *Mini Reviews in Medicinal Chemistry*, 2008, **8**, 436–447.
- 8 K. T. Chung, T. Y. Wong, C. I. Wei, Y. W. Huang, and Y. Lin, *Critical Reviews in Food Science and Nutrition*, 1998, **38**, 421–464.
- 9 T. N. Asquith and L. G. Butler, *Phytochemistry*, 1986, **25**, 1591–1593.
- 10 F. Canon, F. Pat e, V. Cheynier, P. Sarni-Manchado, A. Giuliani, J. P erez, D. Durand, J. Li, and B. Cabane, *Langmuir*, 2013, **29**, 1926–1937.
- 11 M. R. Perez-Gregorio, N. Mateus, and V. de Freitas, *Langmuir*, 2014, **30**, 8528–8537.
- 12 M. R. Perez-Gregorio, N. Mateus, and V. de Freitas, *J. Agric. Food Chem.*, 2014, **62**, 10038–10045.
- 13 Y. Lu and A. Bennick, *Arch. Oral Biol.*, 1998, **43**, 717–728.
- 14 N. Naurato, P. Wong, Y. Lu, K. Wroblewski, and A. Bennick, *J. Agric. Food Chem.*, 1999, **47**, 2229–2234.
- 15 F. Amado, M. Jo ao, C. Lobo, P. Domingues, J. A. Duarte, and R. Vitorino, *Expert. Rev. Proteomics*, 2010, **7**, 709–721.
- 16 M. S. Lamkin and F. G. Oppenheim, *Crit. Rev. Oral Biol. Med.*, 1993, **4**, 251–259.
- 17 P. de Sousa-Pereira, F. Amado, J. Abrantes, R. Ferreira,

- P. J. Esteves, and R. Vitorino, *Arch. Oral Biol.*, 2013, **58**, 451–458.
- 18 J. Muenzer, C. Bildstein, M. Gleason, and D. M. Carlson, *J. Biol. Chem.*, 1979, **254**, 5629–5634.
- 19 E. Jöbstl, J. O'Connell, J. P. A. Fairclough, and M. P. Williamson, *Biomacromolecules*, 2004, **5**, 942–949.
- 20 I. Messana, T. Cabras, E. Pisano, M. T. Sanna, A. Olianias, B. Manconi, M. Pellegrini, G. Paludetti, E. Scarano, A. Fiorita, S. Agostino, A. M. Contucci, L. Calo, P. M. Picciotti, A. Manni, A. Bennick, A. Vitali, C. Fanali, R. Inzitari, and M. Castagnola, *Molecular & Cellular Proteomics*, 2008, **7**, 911–926.
- 21 M. Stubbs, J. Chan, A. Kwan, J. So, U. Barchynsky, M. Rassouli-Rahsti, R. Robinson, and A. Bennick, *Archives of Oral Biology*, 1998, **43**, 753–770.
- 22 A. Bennick, *J. Dent. Res.*, 1987, **66**, 457–461.
- 23 D. M. Carlson, *Critical Reviews in Oral Biology & Medicine*, 1993, **4**, 495–502.
- 24 F. Canon, F. Paté, E. Meudec, T. Marlin, V. Cheynier, A. Giuliani, and P. Sarni-Manchado, *Anal. Bioanal. Chem.*, 2009, **395**, 2535–2545.
- 25 F. Canon, A. Giuliani, F. Paté, and P. Sarni-Manchado, *Anal. Bioanal. Chem.*, 2010, **398**, 815–822.
- 26 F. Canon, R. Ballivian, F. Chiro, R. Antoine, P. Sarni-Manchado, J. Lemoine, and P. Dugourd, *J. Am. Chem. Soc.*, 2011, **133**, 7847–7852.
- 27 F. Groot, R. W. Sanders, O. ter Brake, K. Nazmi, E. C. Veerman, J. G. Bolscher, and B. Berkhout, *J. Virol.*, 2006, **80**, 9236–9243.
- 28 S. Soares, R. Vitorino, H. Osório, A. Fernandes, A. Venâncio, N. Mateus, F. Amado, and V. de Freitas, *J. Agric. Food Chem.*, 2011, **59**, 5535–5547.
- 29 K. Wroblewski, R. Muhandiram, A. Chakrabarty, and A. Bennick, *Eur. J. Biochem.*, 2001, **268**, 4384–4397.
- 30 A. J. Charlton, N. J. Baxter, M. L. Khan, A. J. G. Moir, E. Haslam, A. P. Davies, and M. P. Williamson, *J. Agric. Food Chem.*, 2002, **50**, 1593–1601.
- 31 F. G. Oppenheim, T. Xu, F. M. McMillian, S. M. Levitz, R. D. Diamond, G. D. Offner, and R. F. Troxler, *J. Biol. Chem.*, 1988, **263**, 7472–7477.
- 32 E. J. Helmerhorst, *J. Biol. Chem.*, 2001, **276**, 5643–5649.
- 33 D. Brewer, H. Hunter, and G. Lajoie, *Biochem. Cell. Biol.*, 1998, **76**, 247–256.
- 34 P. A. Raj, E. Marcus, and D. K. Sukumaran, *Biopolymers*, 1998, **45**, 51–67.
- 35 I. Tarascou, K. Barathieu, C. Simon, M. A. Ducasse, Y. André, E. Fouquet, E. J. Dufourc, V. de Freitas, M. Laguerre, and I. Pianet, *Magn. Reson. Chem.*, 2006, **44**, 868–880.
- 36 ChemDraw Ultra 13.0. CambridgeSoft Corporation, 100 Cambridge Park Drive, Cambridge, MA 02140.
- 37 Fred, version 2.2.5. OpenEye Scientific Software Inc., Santa Fe, NM, USA, 2009.
- 38 M. McGann, *J. Chem. Inf. Model.*, 2011, **51**, 578–596.
- 39 AMBER 11. D. A. Case, T. A. Darden, T. E. Cheatham III, C. L. Simmerling, J. Wang, R. E. Duke, R. Luo, R. C. Walker, W. Zhang, K. M. Merz, B. P. Roberts, B. Wang, S. Hayik, A. Roitberg, G. Seabra, I. Kolossvai, K. F. Wong, F. Paesani, J. Vanicek, J. Liu, X. Wu, S. R. Brozell, T. Steinbrecher, H. Gohlke, Q. Cai, X. Ye, J. Wang, M. J. Hsieh, G. Cui, D. R. Roe, D. H. Mathews, M. G. Seetin, C. Sagui, V. Babin, T. Luchko, S. Gusarov, A. Kovalenko, and P. A. Kollman; University of California, San Francisco, 2010.
- 40 D. J. A. T. Davidowitz and R. Benoliel, *Oral Dis.*, 2006, **12**, 420–423.
- 41 Y. Li, F. Heitz, C. L. Grimellec, and R. B. Cole, *Anal. Chem.*, 2005, **77**, 1556–1565.
- 42 The PyMOL Molecular Graphics System, Version 1.3. Schrödinger, LLC, 2010.
- 43 D. S. Wishart, D. Arndt, M. Berjanskii, P. Tang, J. Zhou, and G. Lin, *Nucleic Acids Research*, 2008, **36**, W496–W502.
- 44 Y. Duan, C. Wu, S. Chowdhury, M. C. Lee, G. Xiong, W. Zhang, R. Yang, P. Cieplak, R. Luo, T. Lee, J. Caldwell, J. Wang, and P. Kollman, *J. Comput. Chem.*, 2003, **24**, 1999–2012.
- 45 M. Valiev, E. J. Bylaska, N. Govind, K. Kowalski, T. P. Straatsma, H. J. J. van Dam, D. Wang, J. Nieplocha, E. Apra, T. L. Windus, and W. A. de Jong, *Comput. Phys. Commun.*, 2010, **181**, 1477–1489.
- 46 J. Wang, R. M. Wolf, J. W. Caldwell, P. A. Kollman, and D. A. Case, *J. Comput. Chem.*, 2004, **25**, 1157–1174.
- 47 J. Wang, W. Wang, P. A. Kollman, and D. A. Case, *J. Mol. Graph. Modell.*, 2006, **25**, 247–260.
- 48 W. L. Jorgensen, J. Chandrasekhar, J. D. Madura, R. W. Impey, and M. L. Klein, *J. Chem. Phys.*, 1983, **79**, 926–935.
- 49 M. Rueda, S. G. Kalko, F. J. Luque, and M. Orozco, *J. Am. Chem. Soc.*, 2003, **125**, 8007–8014.
- 50 J. Gidden, A. Ferzoco, E. S. Baker, and M. T. Bowers, *J. Am. Chem. Soc.*, 2004, **126**, 15132–15140.
- 51 M. Rueda, F. J. Luque, and M. Orozco, *J. Am. Chem. Soc.*, 2005, **127**, 11690–11698.
- 52 M. Rueda, F. J. Luque, and M. Orozco, *J. Am. Chem. Soc.*, 2006, **128**, 3608–3619.
- 53 A. Arcella, G. Portella, M. L. Ruiz, R. Eritja, M. Vilaseca, V. Gabelica, and M. Orozco, *J. Am. Chem. Soc.*, 2012, **134**, 6596–6606.
- 54 G. Wang and R. B. Cole, *Org. Mass Spectrom.*, 1994, **29**,

- 419–427.
- 55 Y. Li and R. B. Cole in *Electrospray and MALDI Mass Spectrometry: Fundamentals Instrumentation, Practicalities, and Biological Applications*, ed. R. B. Cole, Vol. 1; Wiley, New York, 2010; chapter 14, pp. 491–534.
- 56 T. Ishii, T. Mori, T. Tanaka, D. Mizuno, R. Yamaji, S. Kumazawa, T. Nakayama, and M. Akagawa, *Free Radical Biology and Medicine*, 2008, **45**, 1384–1394.
- 57 T. Mori, T. Ishii, M. Akagawa, Y. Nakamura, and T. Nakayama, *Bioscience, Biotechnology, and Biochemistry*, 2010, **74**, 2451–2456.
- 58 R. Chen, J. B. Wang, X. Q. Zhang, J. Ren, and C. M. Zeng, *Archives of Biochemistry and Biophysics*, 2011, **507**, 343–349.
- 59 D. Cao, Y. Zhang, H. Zhang, L. Zhong, and X. Qian, *Rapid Commun. Mass Spectrom.*, 2009, **23**, 1147–1157.
- 60 W. Humphrey, A. Dalce, and K. Schulten, *J. Mol. Graphics*, 1996, **14**, 33–38.
- 61 A. E. Hagerman and L. G. Butler, *J. Biol. Chem.*, 1981, **256**, 4494–4497.
- 62 N. J. Baxter, T. H. Lilley, E. Haslam, and M. P. Williamson, *Biochemistry*, 1997, **36**, 5566–5577.
- 63 A. E. Hagerman, K. M. Riedl, G. A. Jones, K. N. Sovik, N. T. Ritchard, P. W. Hartzfeld, and T. L. Riechel, *J. Agric. Food Chem.*, 1998, **46**, 1887–1892.
- 64 N. J. Baxter, T. H. Lilley, E. Haslam, and M. P. Williamson, *Biochemistry*, 1997, **36**, 5566–5577.
- 65 O. Cala, N. Pinaud, C. Simon, E. Fouquet, M. Laguerre, E. J. Dufourc, and I. Pianet, *FASEB J.*, 2010, **24**, 4281–4290.
- 66 O. Cala, S. Fabre, E. Fouquet, E. J. Dufourc, and I. Pianet, *Comptes Rendus Chimie*, 2010, **13**, 449–452.
- 67 I. Pianet, Y. André, M. A. Ducasse, I. Tarascou, J. C. Lartigues, N. Pinaud, E. Fouquet, E. J. Dufourc, and M. Laguerre, *Langmuir*, 2008, **24**, 11027–11035.
- 68 A. K. Dunker, J. D. Lawson, C. J. Brown, R. M. Williams, P. Romero, J. S. Oh, C. J. Oldfield, A. M. Campen, C. M. Ratliff, K. W. Hipps, J. Ausio, M. S. Nissen, R. Reeves, C. Kang, C. R. Kissinger, R. W. Bailey, M. D. Griswold, W. Chiu, E. C. Garner, and Z. Obradovic, *J. Mol. Graph. Model.*, 2001, **19**, 26–59.
- 69 V. N. Uversky, J. R. Gillespie, and A. L. Fink, *Proteins*, 2000, **41**, 415–427.
- 70 S. Vucetic, C. J. Brown, A. K. Dunker, and Z. Obradovic, *Proteins*, 2003, **52**, 573–584.
- 71 G. Bouvignies, P. Markwick, R. Brüschweiler, and M. Blackledge, *J. Am. Chem. Soc.*, 2006, **128**(47), 15100–15101.
- 72 M. Blackledge, *Prog. Nucl. Magn. Reson. Spectrosc.*, 2005, **46**, 23–61.
- 73 A. J. Charlton, E. Haslam, and M. P. Williamson, *J. Am. Chem. Soc.*, 2002, **124**, 9899–9905.
- 74 S. Vergé, T. Richard, S. Moreau, A. Nurich, J. M. Merillon, J. Vercauteren, and J. P. Monti, *Biochim. Biophys. Acta.*, 2002, **1571**, 89–101.
- 75 A. K. Dunker, I. Silman, V. N. Uversky, and J. L. Sussman, *Curr. Opin. Struct. Biol.*, 2008, **18**, 756–764.
- 76 P. Tompa, *Trends Biochem. Sci.*, 2002, **27**, 527–533.
- 77 H. J. Dyson and P. E. Wright, *Nat. Rev. Mol. Cell Biol.*, 2005, **6**, 197–208.
- 78 P. E. Wright and H. J. Dyson, *J. Mol. Biol.*, 1999, **293**, 321–331.
- 79 M. R. Jensen, L. Salmon, G. Nodet, and M. Blackledge, *J. Am. Chem. Soc.*, 2010, **132**, 1270–1272.
- 80 A. De Simone, A. Cavalli, S. T. D. Hsu, W. Vranken, and M. Vendruscolo, *J. Am. Chem. Soc.*, 2009, **131**, 16332–16333.
- 81 O. K. Abou-Zied, N. Al-Lawatia, M. Elstner, and T. B. Steinbrecher, *J. Phys. Chem. B*, 2013, **117**, 1062–1074.
- 82 A. J. Charlton, N. J. Baxter, T. H. Lilley, E. Haslam, C. J. McDonald, and M. P. Williamson, *FEBS Lett.*, 1996, **382**, 289–292.
- 83 V. de Freitas and N. Mateus, *J. Agric. Food Chem.*, 2001, **49**, 940–945.
- 84 M. P. Williamson, *Biochem. J.*, 1994, **297**, 249–260.
- 85 A. K. Dunker, E. Garner, S. Guillot, P. Romero, K. Albrecht, J. Hart, Z. Obradovic, C. Kissinger, and J. E. Villafranca, *Pac. Symp. Biocomput.*, 1998, pp. 473–484.
- 86 P. Sarni-Manchado and V. Cheynier, *J. Mass Spectrom.*, 2002, **37**, 609–616.
- 87 S. Vergé, T. Richard, S. Moreau, S. Richelme-David, J. Vercauteren, J. C. Promé, and J. P. Monti, *Tetrahedron Letters*, 2002, **43**, 2363–2366.

First study correlating experimental mass spectrometry with computational simulations (gas and solution phases) that examines procyanidin binding to Histatin 5.

